PREDICTION OF AERODYNAMIC NOISE FOR CENTRIFUGAL FAN OF AIR-CONDITIONER

Taku IWASE[1], Daiwa SATO[1], Hideshi OBARA[2], Hiroyasu YONEYAMA[2], Tetsushi KISHITANI[2], Yoshinobu YAMADE[3], Chisachi KATO[3]

[1] *Hitachi, Ltd., Hitachi Research Laboratory, 832-2, Horiguchi, Hitachinaka, Ibaraki, 312-0034, Japan*

[2] *Hitachi Appliances, Inc., 390, Muramatsu, Shimizu, Shizuoka, 424-0926, Japan*

[3] *Tokyo University, 4-6-1, Komaba, Meguro, Tokyo, 153-8505, Japan*

SUMMARY

Flow fields and aerodynamic noise in centrifugal fans of air-conditioners were calculated by large eddy simulation. The intended centrifugal fans were two types and they had different blade shapes. Calculations were implemented by using K computer, which is Japanese national super computer. We compared 60 million grids (60M-grid) and 500 million grids (500M-grid) calculation results to investigate the influence of grid resolution on the prediction accuracy. The prediction accuracy of the aerodynamic noise by 500M-grid was improved compared to 60M-grid calculation results. The proper capturing of the streaks contributed to the improvement of the prediction accuracy.

INTRODUCTION

Development of silent air-conditioners is one of the most important requirements in recent life-styles since the aerodynamic noise from fans accounts for a large percentage of the overall noise from air-conditioners. Therefore, the development of silent fans would contribute to reduce the noise levels of air-conditioners.

Figure 1 shows a schematic structure of an indoor unit of an air-conditioner. The centrifugal fan has a very complicated flow field near the bell mouth and the shroud. The centrifugal fans have been mainly developed by using experimental methods. Predictions of aerodynamic noise were based on estimates from static flow field characteristics and experimental coefficients [1]. However, it is difficult to develop radically silent fans by using traditional methods any more. We therefore need

new methods of predicting aerodynamic noise. Computational fluid dynamics (CFD) is a powerful tool for solving these needs. Many researchers have recently studied flow fields by using large eddy simulation (LES) [2][3][4][5][6][7]. However, as far as we know there are few study cases about high accurate prediction of aerodynamic noise by using more than 100 million grids.

The goal of our study was aimed at developing methods of high accurate prediction of aerodynamic noise. Flow fields and the aerodynamic noise in the centrifugal fan for the indoor unit of the air-conditioner were calculated by LES with the aim of predicting fan performance and aerodynamic noise in this study. We actually compared 60 million grid [60M-grid] and 500 million grid [500M-grid] calculation results to investigate the influence of grid resolution on the prediction accuracy.

METHOD OF NUMERICAL SIMULATION

Test fan

The centrifugal fan used in the indoor unit of air-conditioner was intended in this study. As shown in Figure 1, there is a heat exchanger outside the impeller in the indoor unit of the air-conditioner. The unit does not have a volute and outlet guide vanes. The air enters from a grill and a filter. The air passes the heat exchanger, and discharges from flow paths.

Figure 2 shows the intended centrifugal fans. The intended centrifugal fans were two types, type-A and type-B. They had different blade shapes and fan performances. The impeller diameter was 490 mm, and the number of blade was seven. The type-A fan had inclined two-dimensional blades. The type-B fan had three-dimensional blades. The static pressure rise of the type-B fan at the specified flow rate was smaller than that of the type-A fan. The fan efficiency of the type-B fan was higher than that of the type-A fan. The aerodynamic noise of the type-B fan was almost the same as that of the type-A fan. The fan had a bell mouth overlapped with a shroud of an impeller. As a result, a leakage flow occurred between the bell mouth and the shroud. The centrifugal fan therefore had a very complicated flow field near the bell mouth and the shroud.

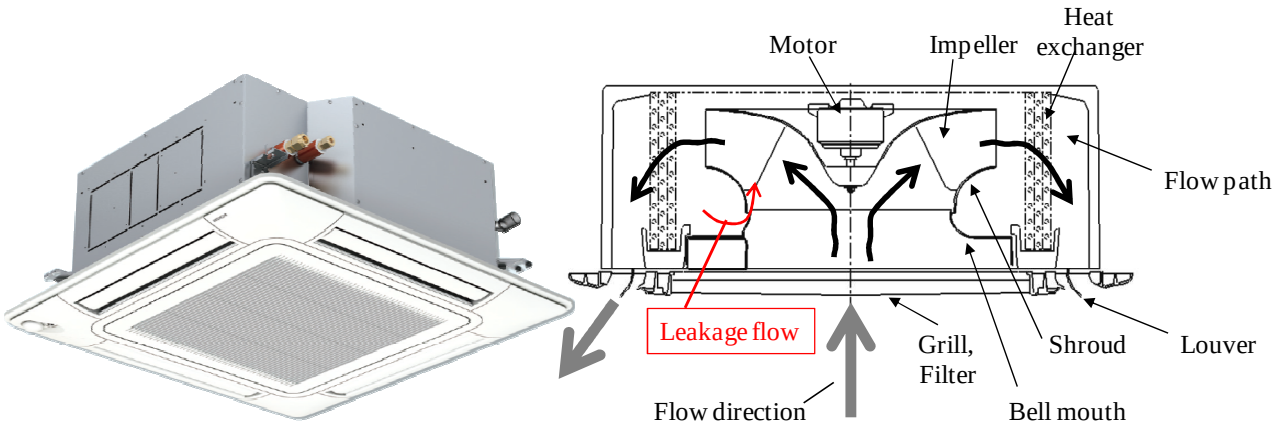

Figure 1: Schematic structure of an indoor unit of an air-conditioner

(a) Type-A fan (b) Type-B fan

Figure 2: The intended centrifugal fans

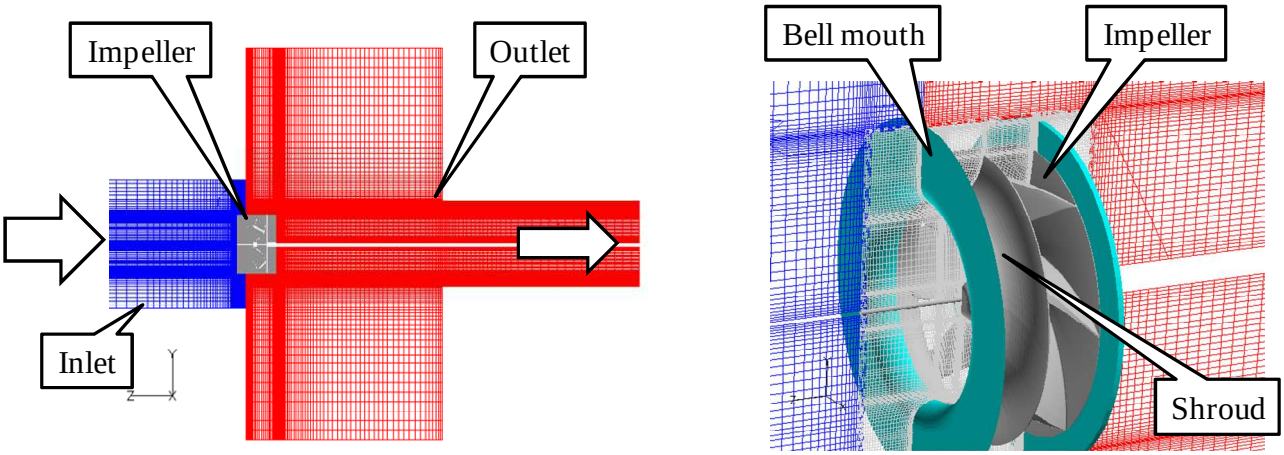

(a) Construction of computational grids (b) Grids around impeller

Figure 3: Computational grid model

Large eddy simulation

The numerical simulation code employed throughout the LES was called FrontFlow/blue (FFB), which was developed by Kato et al. and successfully used for several applications [3][4][5][7]. The code was based on the finite element discretization of filtered incompressible continuity and Navier Stokes equations. The dynamic Smagorinsky model was used as a sub-grid scale model.

The interaction between the rotating impeller and the stationary parts was taken into account by dynamically oversetting the grids from multiple frames of reference [8]. Each grid part included appropriate margins of overlap with their neighboring grid parts downstream and upstream. The values for static pressure and velocity components in the margin were interpolated in corresponding neighboring elements at each time step.

Computational Conditions

Figure 3 shows a computational grid model. The experimental apparatus as shown in Figure 5 was modeled. The heat exchanger was therefore not modeled in the computation. The computational model consisted of three parts, i.e., the inlet, impeller, and outlet parts. The impeller part was in the rotating frame of reference. The inlet and the outlet parts were in the stationary frames. The grid

was composed of hexahedral elements. An additional pipe was added to the end of the cylinder for the outlet part to stabilize calculations.

In this study, we compared 60 million grids (60M-grid) and 500 million grids (500M-grid) calculation results to investigate the influence of grid resolution on the prediction accuracy. Table 1 lists the number of grid elements. Figure 4 shows the grids of blade surfaces of the 60M-grid. The 500M-grid was generated by refining the 60M-grid. FFB solver automatically divided twice the element of the 60M-grid in each direction. The number of grid elements of the 500M-grid was therefore eight times as that of the 60M-grid. The y+ of the 500M-grid was designed to be y+ = 6 on the blade surface. Figure 4 shows the grid surface of the impellers of the 60M-grid.

The calculation conditions of flow rate and rotational speed were 22 m^3/min and 570 rpm. The flow rate of the 22 m^3/min was the specified flow rate of the air-conditioner. The time increments were 2.57×10^{-5} second with 60M-grid calculation and 1.28×10^{-5} second with 500M-grid calculation. These time increments corresponded to 4,096 time steps and 8,192 time steps for one revolution of the impeller. FFB used in the present study can calculate stably when CFL (Courant-Friedrichs-Lewy condition) was lower than 5. The time increment was decided from this CFL restriction.

Table 1: The number of grid elements

Grid	Domain	Type-A	Type-B
60M-grid	Inlet	846,720	844,976
	Impeller	55,629,014	63,086,716
	Outlet	4,385,664	4,407,936
	Total	60,861,398	68,339,628
500M-grid	Inlet	6,773,760	6,759,808
	Impeller	445,032,112	504,693,728
	Outlet	35,085,312	35,263,488
	Total	486,891,184	546,717,024

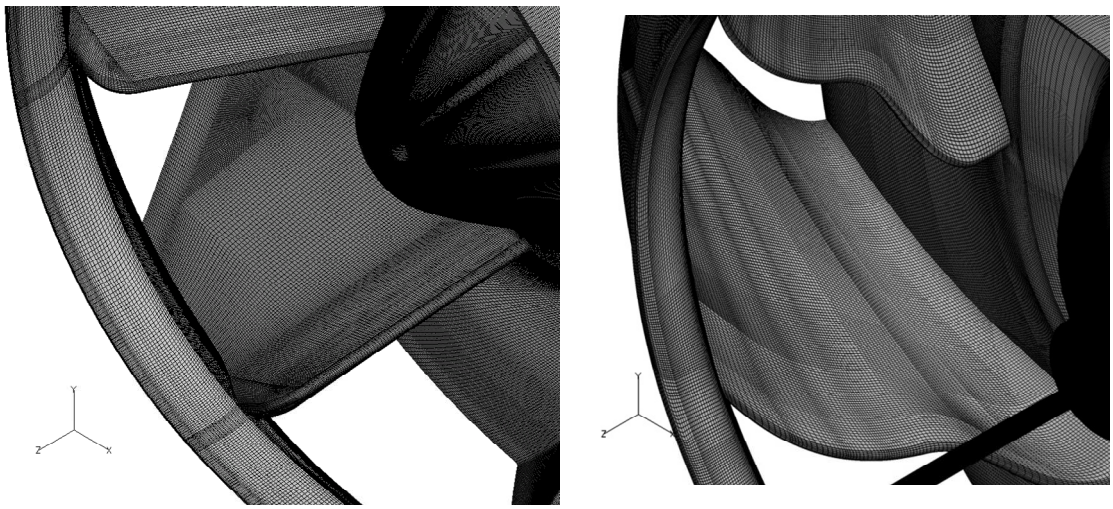

(a) Type-A fan (b) Type-B fan

Figure 4: The grid surface of the impellers of the 60M-grid

Static pressure rise was monitored during calculation. In the 60M-grid calculation, the converged solution of static pressure rise was obtained after 16 revolutions. First, static condition calculation was implemented for 4 revolutions to initialize the flow field. Then, dynamic condition calculation was done for 12 revolutions. The 500M-grid calculation was started by using the final flow field data of the 60M-grid. The 500M-grid calculation was done for 6 revolutions. The 60M-grid computational time for one revolution was about 20 hours by using 512 cores of super technical server, HITACHI SR16000. The 500M-grid was about 20 hours by using 8,192 cores of K computer, which is Japanese national super computer developed for high performance computing.

The calculated results were sampled during 4 revolutions of the impeller after the converged solution. The required computational resources of 4 revolutions calculation, which are obtained for the product of cores and hours (i.e., core-hours), were 40,960 core-hours in the 60M-grid and 655,360 core-hours in the 500M-grid. The data of velocities in three direction and static pressure were stored during the calculation in each grid element. After the calculation, FFB solver automatically outputs three flow field data, an averaged data, a temporary data, and a root mean square data.

Aerodynamic noise was calculated with Curle's equation [9] defined by the following equation (1). Here, ρ is the instant density, ρ_0 is the density in a uniform medium at rest, and c_0 is the sound speed. x_i is the observation point, r is the distance between the observation point and the sound source, t is the time, and n_i is the outward normal vector on solid surface S. p represents static pressure fluctuations on solid surface S. The aerodynamic noise was calculated in the same point as measured one, 1 m away from the impeller. The sound source was assumed to be acoustically compact. We therefore estimated that the upper limit of the frequency was 1,550 Hz, which was decided from a pitch size of the blade.

$$\rho - \rho_0 = \frac{1}{4\pi c_0^{\,3}} \frac{x_i}{r^2} \frac{\partial}{\partial t} \int_s n_i \, p \, dS \qquad (1)$$

We also considered influence of the size of the anechoic chamber room on the measured aerodynamic noise. The 136 Hz corresponds to the length of two sound waves in the anechoic chamber room size of 5 meters. The experimental sound pressure spectrums greater than 136 Hz were therefore available in this paper. Accordingly, the estimated frequency range was between 136 Hz and 1,550 Hz.

EXPERIMENTAL APPARATUS AND PROCEDURES

Fan Performance Test

Fan performance was measured to verify the calculated results. Fan performance in this study denoted the flow rate, static pressure rise, shaft power, and aerodynamic noise. Figure 5 schematically shows the experimental apparatus for measuring flow rate, static pressure rise, and shaft power. We used a double chamber complied with JIS B 8330, Japanese Industrial Standards "Testing methods for turbo-fans."

The measurement of aerodynamic noise was conducted in an anechoic chamber room at Hitachi Research Laboratory. The sizes of the anechoic chamber room were 5 meters long, 6 meters wide, 5 meters high. Figure 6 shows a photograph of measurement of aerodynamic noise. A microphone (B&K Type 4190) was placed 1 m away from the impeller. The measurement accuracy of the sound pressure spectrum was ± 0.2 dB from specification of the microphone. The elapsed time was 10 second. An Hanning window function was applied to all measured data sets to perform a fast Fourier transform.

Measurements of Velocity Distributions

We measured time-averaged velocity distributions and velocity fluctuations downstream of the blade to verify the calculated results. The measured flow rate and rotational speed were 22 m^3/min and 570 rpm, which were the same as those for calculations.

The time-averaged velocity distributions were measured with 5-hole type pitot tube. Figure 7 shows a photograph of measurement of the time-averaged velocity distributions and an illustration of measurement points. The pitot tube was placed at 120 % impeller diameter *D*. The pitot tube was traversed along the axial direction. The pitot tube measurement accuracy was maximum ± 9 % from specification of differential pressure transmitter.

The velocity fluctuations were measured with an I-type hotwire probe (KANOMAX, 0251R-T5). Figure 8 shows a photograph of measurement of the velocity fluctuations. Figure 7 (b) also shows an illustration of measurement points. The hotwire probes were placed at 105 % and 120 % impeller diameters, and were traversed along the axial direction. The hotwire probe was calibrated previously with the range of measurement velocity. Before the measurement by the hotwire probe, we checked the flow direction of the absolute velocities by using a tuft. When we measured the absolute velocities, The hotwire probe was fixed in the flow direction. The velocity fluctuations were evaluated by the root mean square.

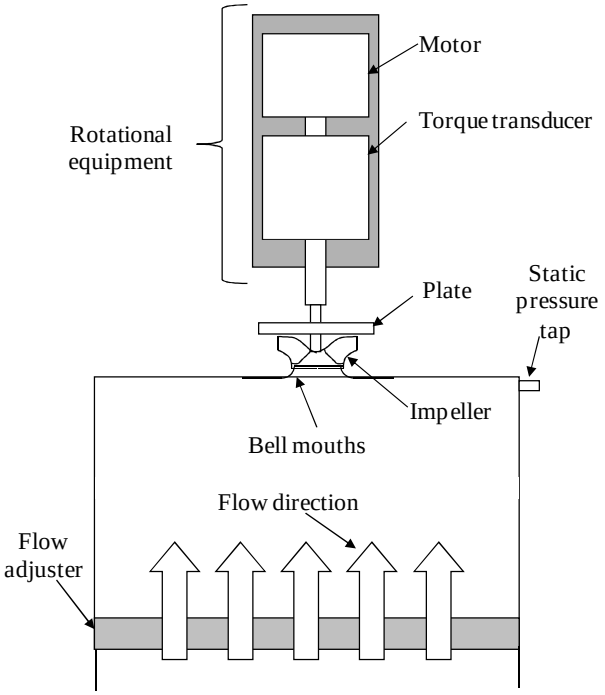

Figure 5: The experimental apparatus

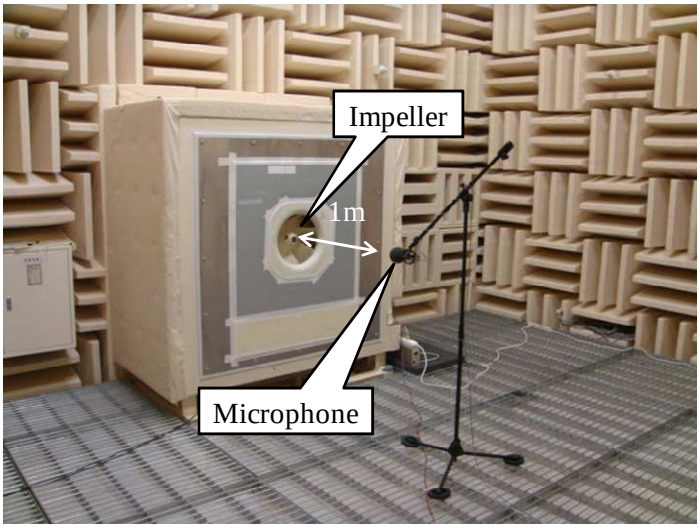

Figure 6: Photograph of measurement of aerodynamic noise

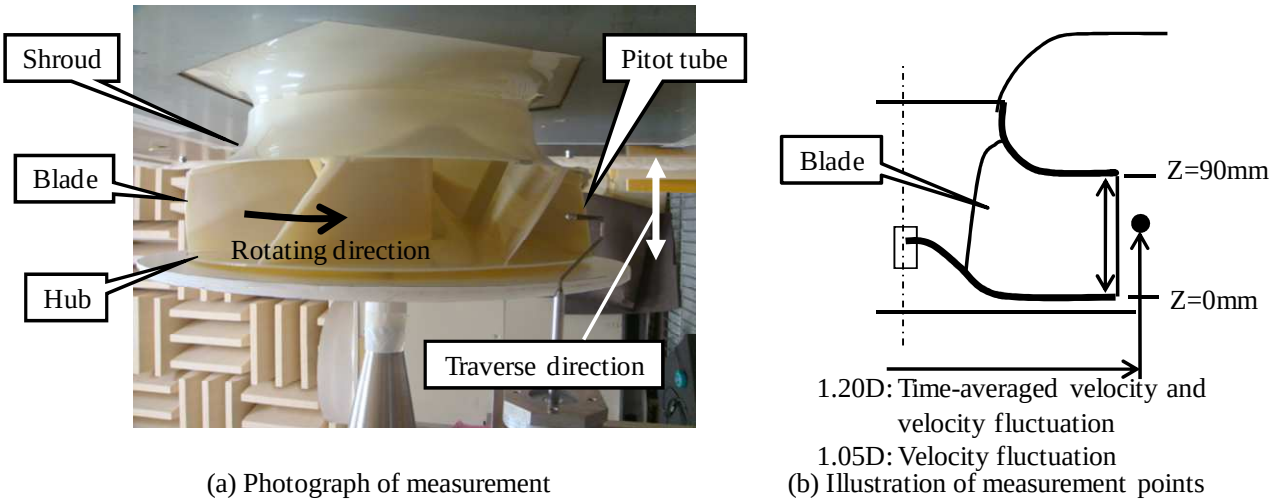

(a) Photograph of measurement (b) Illustration of measurement points

Figure 7: Photograph of measurement of the time-averaged velocity distributions and an illustration of measurement points

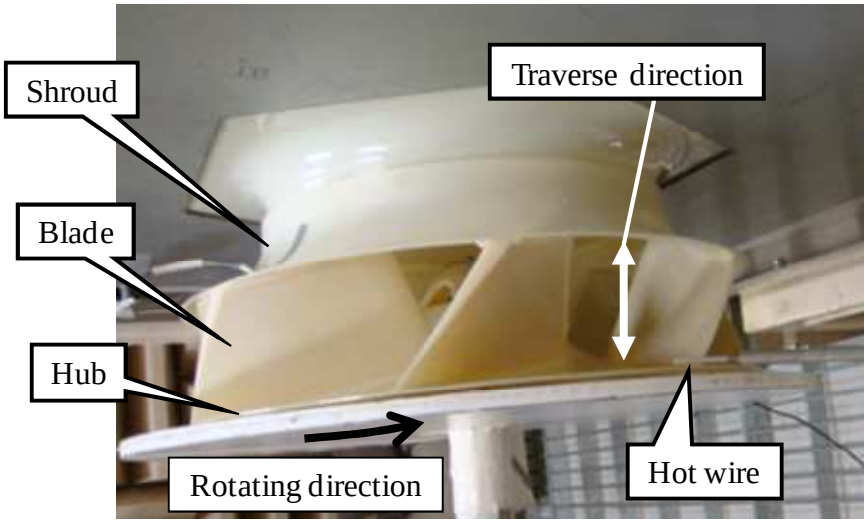

Figure 8: Photograph of measurement of the velocity fluctuations.

RESULTS AND DISCUSSION

Validity of Numerical Simulations

We compared calculated and experimental results for assessment of the LES quality, and to investigate the influence of grid resolution on the prediction accuracy. We evaluated the fan performance, time-averaged velocity distributions, velocity fluctuations, and aerodynamic noise of the type-A fan. We also compared fan performance and aerodynamic noise of the type-B fan.

Figure 9 compares the fan performance. The shaft power was normalized by the experimental shaft power at the calculated flow rate. The calculation results by the 60M-grid and the 500M-grid agreed with the experimental results within the accuracy of ±10%. Figure 10 compared the time-averaged velocity distributions of the type-A fan. The type-A fan had two dimensional inclined blades due to constraints of production. There was therefore low velocity region near the shroud, though the compared 22 m^3/min was the specified flow rate. The radial and tangential velocities near the hub were larger than those near the shroud.

The flow rate of blade-to-blade was larger than the 22 m^3/min caused by the leakage flow through the gap of the shroud and the bell mouth. In Figure 10, the experimental averaged radial velocity of 3.1 m/s was therefore larger than the averaged radial velocity according to $C_r = Q/(\pi Db) = (22/60)/(\pi \times 0.49 \times 0.09) = 2.6$ m/s. Here, D is the impeller diameter, and b is the width of blade exit.

In Figure 10, the calculated radial and tangential velocities by the 500M-grid increased near the shroud as compared to those by the 60M-grid. Moreover, the calculated axial velocity by the 500M-grid decreased as compared to that by the 60M-grid. The calculated time-averaged velocity distributions by the 500M-grid therefore agreed well with the experimental results. Figure 10 (d) also compares the absolute velocities measured by the pitot tube and the hotwire probe in order to investigate the hot wire measurement accuracy. The experimental results of the hot wire probe were different from those of the pitot tube within ± 8 %. The error range of ± 8 % was almost the same as the measurement accuracy of pitot tube.

Figure 11 compares the velocity fluctuations of the type-A fan. In Figure 11, the distribution of the velocity fluctuation qualitatively captured though the calculated results were overestimated against the experimental results. The calculated velocity fluctuations by the 500M-grid decreased as compared to those by the 60M-grid. The calculation accuracy by the 500M-grid was improved.

Figure 12(a) compares the aerodynamic noise of the type-A fan. The sound pressure spectrums were evaluated by no frequency weighting characteristics, as called F-weighting, for comparison to calculated results. The estimated range of frequency was from 136 Hz to 1,550 Hz. The overestimations of the sound pressure levels near 800 Hz with the 60M-grid calculation were suppressed by the 500M-grid calculation. Moreover, the underestimations of the sound pressure levels greater than 900 Hz were suppressed by the 500M-grid calculation.

Figure 12(b) compares the aerodynamic noise of the type-B fan. The calculated sound pressure levels of the 60M-grid were overestimated. The calculated sound pressure levels of the 500M-grid agreed with the experimental results in the whole range of the measured data. The tendency of over and under estimation of the type-B fan was different from that of the type-A fan. The analysis of this reason was future works.

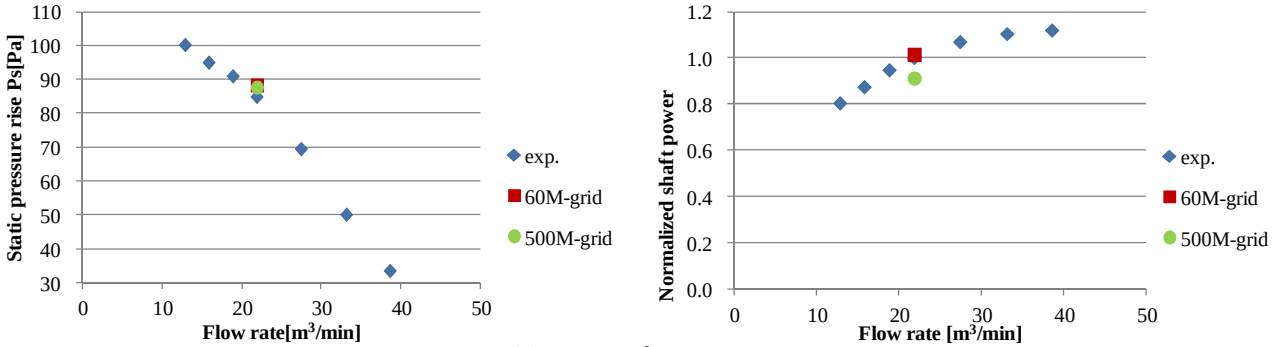

(a) Type-A fan

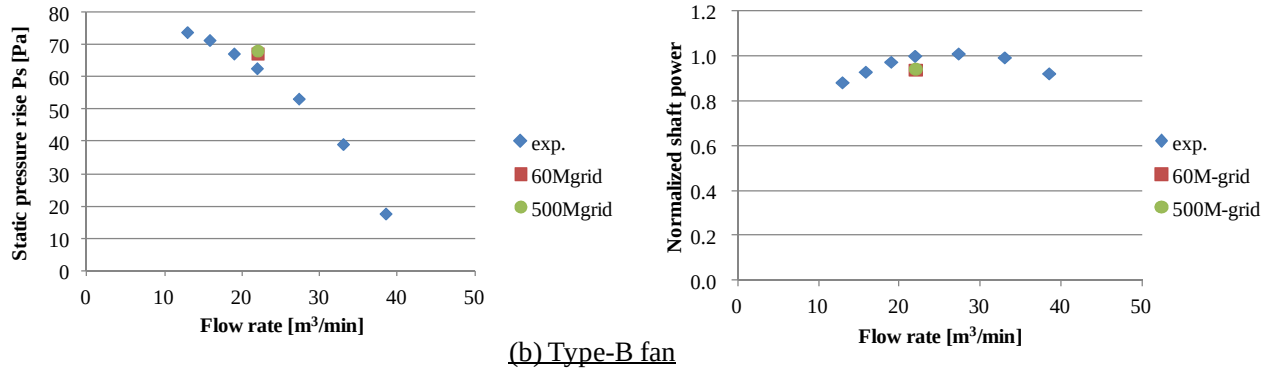

(b) Type-B fan

Figure 9: Comparison of the fan performance

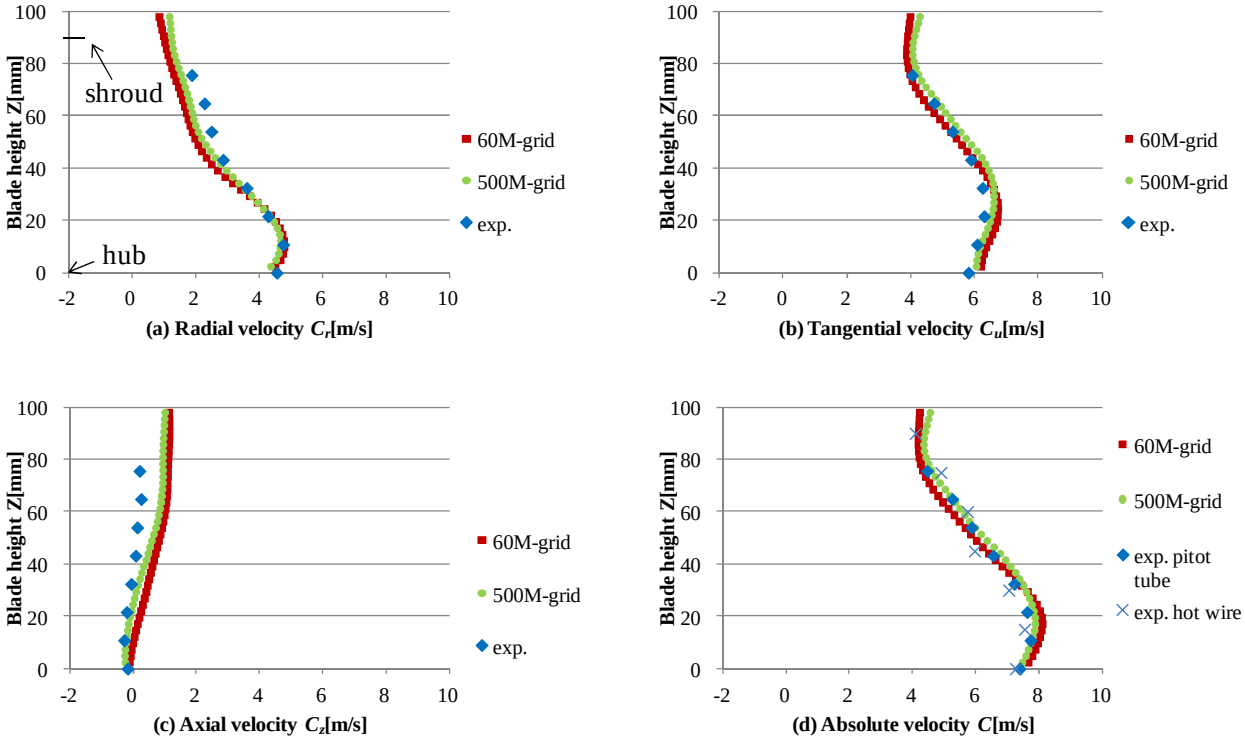

Figure 10: Comparison of the time-averaged velocity distributions of the type-A fan

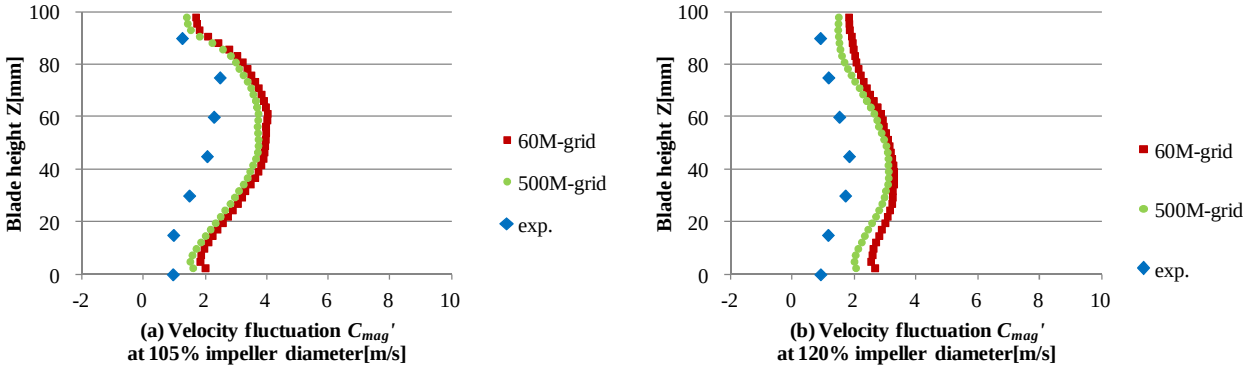

Figure 11: Comparison of the velocity fluctuations of the type-A fan

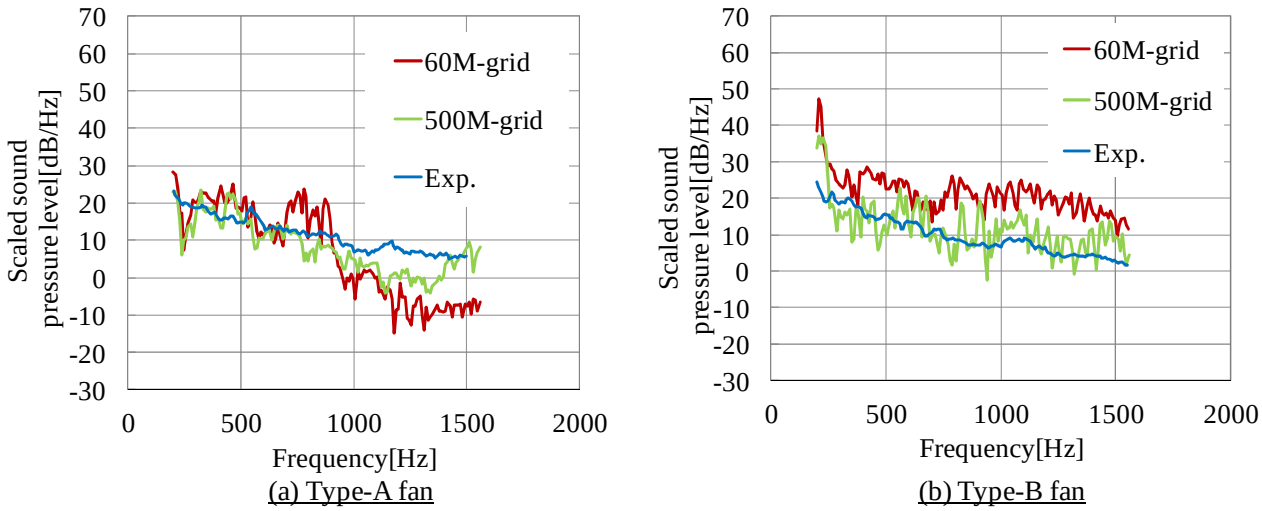

Figure 12: Comparison of the aerodynamic noise of the type-A fan and the type-B fan

Streaks on Blade Surfaces

Figure 13 shows the instantaneous vortices on the blades. The vortices of the nearest element to the surfaces were shown, and were normalized by the impeller diameter and the peripheral velocity at trailing edge. We confirmed that there were streaks having high values of vortices. The streak was a vortex, which had a vortex core parallel to the flow direction near the wall. The steak was considered to be a representative source of aerodynamic noise.

In both cases of the 60M-grid and the 500M-grid, we confirmed the some streaks on the blade surface in span wise direction. The resolution of the 500M-grid was twice as that of the 60Mgrid. Size of streaks by the 500M-grid became smaller. Compared in the circle mark X and Y, the 500M-grid calculation actually captured finer streaks than those of the 60M-grid. As a result, number of captured streaks on the blade by 500M-grid increased as compared to those by 60M-grid. The proper capturing of the streaks contributed to the improvement of the prediction accuracy. We therefore confirmed that high performance computing by K computer was effective for improvement of the prediction of the aerodynamic noise for the centrifugal fan of the air-conditioner.

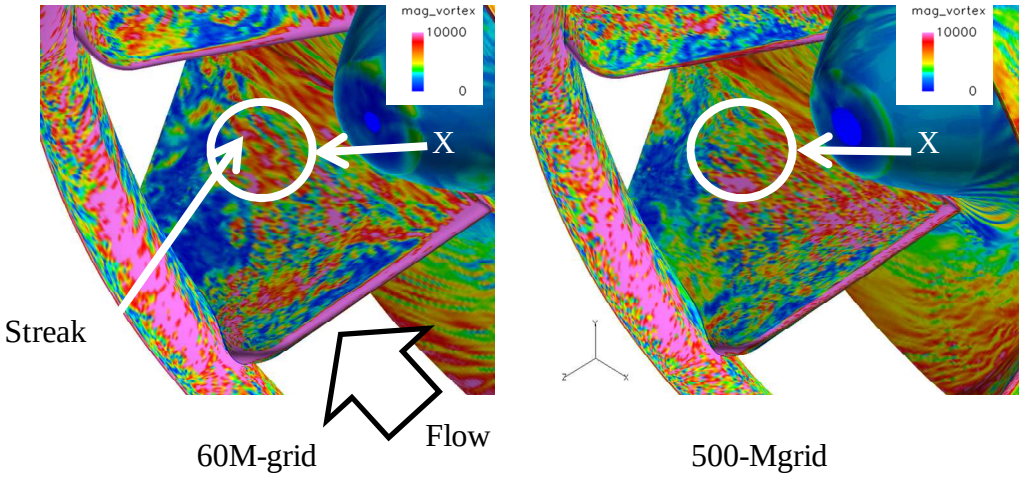

(a) Type-A fan

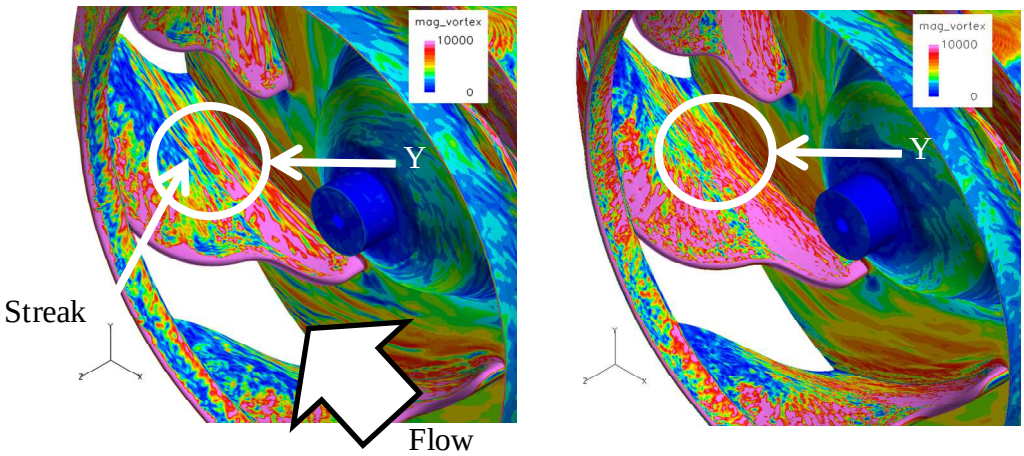

(b) Type-B fan

Figure 13: Instantaneous vortices on the blades

CONCLUSIONS

Flow fields and aerodynamic noise in the centrifugal fan for the indoor units of air-conditioners were calculated by LES for predicting the fan performance and aerodynamic noise in this study. We compared 60 million grids (60M-grid) and 500 million grids (500M-grid) calculation results to investigate the influence of grid resolution on the prediction accuracy. The main results were summarized as follows:

The fan performance and time-averaged velocity distributions agreed reasonably with the experimental results and the distributions of velocity fluctuations were captured qualitatively, and the over and under estimations of sound pressure were therefore suppressed by improving the grid resolution from the 60M-grid to the 500M-grid.

The size of streak by the 500M-grid became smaller. The number of captured streaks on the blade by 500M-grid increased as compared to those by 60M-grid. The proper capturing of the streaks contributed to improvement of calculation results. We therefore confirmed that high performance computing by K computer was effective for improvement of the prediction of the aerodynamic noise for the centrifugal fan of the air-conditioner.

REFERENCES

[1] Watanabe, M., Takada, Y., Sato, and R., Otaguro, T., "*Prediction of Aerodynamic Noise of Fans*", Transactions of the Japan Society of Mechanical Engineers, Series B, Vol.66, No.642, pp.453-459, **2000**.

[2] Jang, C. M., Furukawa, M., and Inoue, M., "*Analysis of Vortical Flow Field in a Propeller Fan by LDV Measurements and LES Part 1: Three-Dimensional Vortical Flow Structures*", Transactions of the ASME, Journal of Fluids Engineering, Vol.123, No.4, pp.748-754, **2001**.

[3] Yamade, Y., Kato, C., Shimizu, H., and Nishioka, T., "*Large Eddy Simulation and Acoustical Analysis for Prediction on Aeroacoustics Noise Radiated From an Axial-flow Fan*", Proceedings of the ASME Fluids Engineering Conference, FEDSM2006-98303, Miami, Florida, USA, **2006**.

[4] Reese, H., Carolus, T., and Kato, C., "*Numerical prediction of the aeroacoustique sound sources in a low pressure axial fan with inflow distortion*", Proceedings of Fan Noise 2007 Symposium, Lyon, France, **2007**.

[5] Hamada, S., Nakashima, S., Kato, C., Yamade, Y., "*Aerodynamic noise simulation of a propeller fan by large eddy simulation*", Proceedings of 5th Joint ASME/JSME Fluids Engineering Conference, FEDSM2007-37145, San Diego, California, USA, **2007**.

[6] Jeon, W. H., Kobayashi, T. Kodama. T., Hamada, S., "*Study on the CFD method for noise source identification and aeroacoustic analysis of an axial fan*", inter-noise 2011, Osaka, Japan, **2011**.

[7] Iwase, T., Kishitani, T, and Furukawa, M., "*Influence of blade number on aerodynamic noise of propeller fans for outdoor unit of air-conditioner*", Proceedings of Fan 2012, Senlis, France, **2012**.

[8] Kato, C., Kaiho, M., and Manabe, A., "*An Overset Finite Element Large Eddy Simulation Method with Application to Turbomachinery and Aeroacoustics*", Transactions of the ASME, Journal of Applied Mechanics, Vol.70, pp.32-43, **2003**.

[9] Curle, N., "*The Influence of Solid Boundaries upon Aerodynamic Sound*", Proceedings of the Royal Society of London Series A, Mechanical and Physical Sciences, Vol.231, No.1187, pp.505-514, **1955**.

ACKNOWLEDGMENT

This research used computational resources of the K computer provided by the RIKEN Advanced Institute for Computational Science through the HPCI System Research project (Project ID:hp130043).

NOMENCLATURE

LES	Large Eddy Simulation
FFB	FrontFlow/blue
CFL	Courant-Friedrichs-Lewy condition

C_r	Radial velocity [m/s]
C_u	Tangential velocity [m/s]
C_z	Axial velocity [m/s]
C_{mag}'	Absolute velocity fluctuation [m/s]
C	Absolute velocity [m/s]